View metadata, citation and similar papers at core.ac.uk

brought to you by CORE

provided by Elsevier - Publisher Connector

tion was present in 4 patients. Total serum creatine kinase (range 176 to 1,573 U/l, mean: 700 ± 449 U/l, normal <225 U/l), creatine kinase MB fraction (range 15.1 to 174 ng/ml, mean 61 ± 53 ng/ml, normal <9.0 ng/ml), and serum troponin-T (range 0.46 to 3.23 ng/ml, mean 1.401 ± 0.95 ng/ml, normal <0.1 ng/ml) levels were elevated in 7, 8, and 8 patients, respectively. Evidence for recent streptococcal infection was obtained from antistreptolysin O titer in 7 patients (range 392 to 2,364 IU/ml, mean 851 ± 745 IU/ml, normal <200 IU/ml), positive throat culture in 3 patients, and positive rapid streptococcal antigen test in 1 patient. Emergent invasive (n = 6) or computed tomographic (n = 1) angiography showed normal epicardial coronary arteries. Coronary angiography was not performed in a 20-year-old man with recurrent SPAM in whom normal coronary arteries had been demonstrated during a similar episode 6 years earlier. CMR was performed within 2 days of presentation in 7 patients. All patients showed a characteristic subepicardial LGE (3 to 8 segments, mean 5 ± 1.6 of 17 LV segments) (Figs. 1A and 1B); LV ejection fraction ranged from 40% to 64% (mean 53 ± 8%) and was mildly reduced in 4 patients. Resting myocardial perfusion was normal in all. Follow-up CMR was performed 12 ± 7 months after initial presentation in 6 patients. In 5 patients, LV systolic function improved, but in aggregate, LV function improvement was not statistically significant (LV ejection fraction: 61 ± 6 vs. 55 ± 5 at baseline, 95% confidence interval [CI]: −2.5 to 13.2; p = 0.14) and in all patients end-diastolic diameter showed a trend to improvement (50 ± 5 mm vs. 53 ± 5 mm at baseline, 95% CI: −6.3 to 0.3; p = 0.06). Follow-up CMR showed fewer LV segments with LGE (2 ± 1 vs. 5 ± 1.6 segment at baseline, 95% CI: −2.1 to −3.9; p = 0.0004) (Figs. 1C and 1D). Patients received antibiotics and nonsteroidal anti-inflammatory agents; beta-adrenergic blocking agents were given to 5 patients with LV systolic dysfunction. All patients showed clinical improvement during 2 to 3 (mean 2.4 ± 0.7) days of hospitalization and had complete resolution of clinical symptoms at follow-up. This report is limited by the fact that T2-weighted CMR imaging was not performed.

This report provides clinical, ECG, laboratory, coronary angiographic, and echocardiographic features of SPAM, wherein myocarditis was verified by CMR tissue characterization. Despite the small number of patients, the present report emphasizes several important clinical considerations. SPAM may not be as infrequent as previously recognized. It may remain a consideration in the differential diagnosis of acute STEMI, especially in young patients without traditional risk factors for coronary artery disease (1,2). Furthermore, this small series suggests that nonrheumatic presentation of SPAM may resolve upon antibiotic therapy. However, it is not clear whether chronic antibiotic prophylaxis would be necessary in patients who recover from SPAM, especially in those with frequent exposure to streptococcal infection. It is also not clear whether such an initial interaction is a prelude to development of rheumatic fever, especially since the binding of group A streptococci (GAS) to collagen has been proposed, similar to a well-conserved virulence trait of *Staphylococcus aureus*.

Rasoul Mokabberi, MD, Jamshid Shirani, MD, Afsaneh Haftbaradaran M., B. Dennis Go, MD, William Schiavone, DO*

*Geisinger Medical Center, Department of Cardiology, 100 North Academy Avenue, Danville, Pennsylvania 17822-2775.
E-mail: waschiavone@geisinger.edu

doi:10.1016/j.jcmg.2010.05.012

REFERENCES

1. Narula J, Khaw BA, Dec GW Jr., et al. Recognition of acute myocarditis masquerading as acute myocardial infarction. N Engl J Med 1993;328:100–4.
2. Mahrholdt H, Goedecke C, Wagner A, et al. Cardiovascular magnetic resonance assessment of human myocarditis: a comparison to histology and molecular pathology. Circulation 2004;109:1250–8.

Lipid-Rich Obstructive Coronary Lesions

Is Plaque Characterization Important?

We read with interest the high-risk nature of atherosclerotic plaques harboring circumferential necrotic cores (termed *napkin-ring* necrotic cores [1]), their possible association with optical coherence tomography-verified thin fibrous caps (2), and the likelihood of poor outcomes after coronary intervention (3). We, by using multimodality imaging, present the importance of clinical recognition of such plaques, especially if an intervention is planned.

An 85-year-old woman with hypertension and hyperlipidemia on pharmacologic therapy underwent an exercise stress test after reporting atypical chest pain. The stress test showed normal electrocardiographic response to exercise, normal ventricular function, and a small apical perfusion defect. The coronary computed tomography angiography (CTA) revealed a calcium score of zero and a significant stenosis in the mid-left anterior descending artery, subsequently confirmed by selective coronary angiography. CTA demonstrated a positively remodeled (PR) (remodeling index = 1.7), low attenuation (20 ± 10 Hounsfield units) plaque (LAP) (Fig. 1). Intravascular ultrasound demonstrated a minimal luminal area of 2.5 mm^2 and a plaque burden of 79% (Fig. 2A and 2B). Near-infrared spectroscopy (NIRS) (4) confirmed a circumferential lipid-rich lesion (Fig. 2C). The patient underwent percutaneous intervention with a drug-eluting stent that was complicated by transient no-reflow and a periprocedural myocardial infarction (peak troponin, 8.1 ng/ml) (Fig. 3). This case highlights the complementary findings suggestive of a high-risk coronary plaque obtained from different imaging modalities. PR and LAP on CTA, a minimal luminal area <4 mm^2 or >70% cross-sectional plaque burden, and napkin-ring lipid-rich lesion on NIRS usually associated with high-risk plaques also demonstrate the increased risk of distal embolization and no-reflow after intervention (5). The subsequent hospital course was uneventful, and the patient was discharged 3 days after the procedure. Now that we are able to define the composition of plaques by noninvasive and intravascular imaging modalities, it becomes necessary to design a clinical

JACC: CARDIOVASCULAR IMAGING, VOL. 3, NO. 8, 2010
AUGUST 2010:892–6

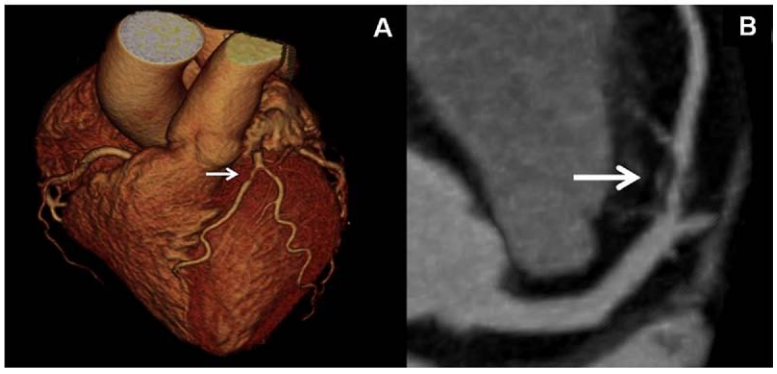

Figure 1. Coronary CT Angiography Findings

Volume rendered **(A)** and multiplanar reformatted **(B)** images demonstrating a severe stenosis in the mid-left anterior descending artery **(arrows)**.

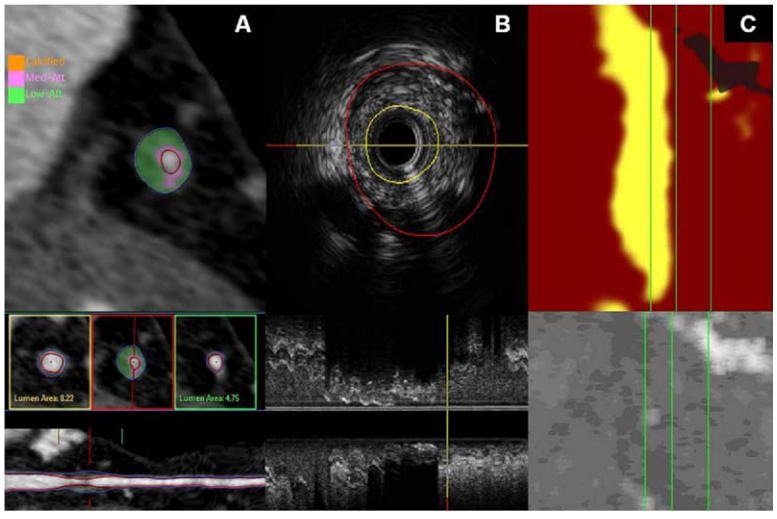

Figure 2. Quantitative Multimodality Imaging of Lipid-Rich Obstructive Coronary Lesion

(A) Computed tomography angiography demonstrates eccentric remodeling and low plaque attenuation **(green)**. **(B)** Intravascular ultrasound confirms severe stenosis and plaque burden. **(C)** Near-infrared spectroscopy indicates high lipid content **(yellow)**.

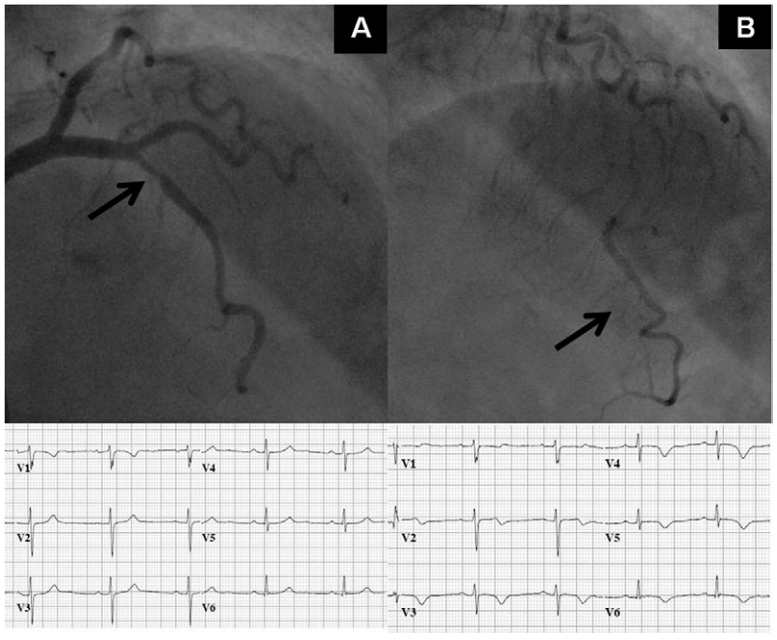

Figure 3. Invasive Coronary Angiography

Catheterization confirmed the stenosis in the mid-left anterior descending coronary artery **(A)** and no-reflow phenomenon after stent placement **(B)**. Electrocardiographic changes are also shown.

investigation to address whether lipid-rich obstructive lesions should be treated differently for revascularization.

Leticia Fernandez-Friera, MD, Ana Garcia-Alvarez, MD, Alaitz Romero, MD, Valentín Fuster, PhD, MD, Mario García, MD, Pedro R. Moreno, MD, Javier Sanz, MD*

*Cardiovascular Institute, Mount Sinai Hospital, One Gustave L. Levy Place, Box 1030, New York, New York 10029. *E-mail: Javier.Sanz@mssm.edu*

doi:10.1016/j.jcmg.2010.06.009

Dr. Moreno is the founder of and a stockholder in InfraReDx, Inc.

REFERENCES

1. Narula J, Achenbach S. Napkin-ring necrotic cores: defining circumferential extent of necrotic cores in unstable plaques. J Am Coll Cardiol Img 2009;2:1436–8.
2. Kashiwagi M, Tanaka A, Kitabata H, et al. Feasibility of noninvasive assessment of thin-cap fibroatheroma by multidetector computed tomography. J Am Coll Cardiol Img 2009;2:1412–9.
3. Goldstein JA, Grines C, Fischell T, et al. Coronary embolization following balloon dilation of lipid-core plaques. J Am Coll Cardiol Img 2009;2:1420–4.
4. Waxman S, Dixon SR, L'Allier P, et al. In vivo validation of a catheter-based near-infrared spectroscopy system for detection of lipid core coronary plaques: initial results of the SPECTACL study. J Am Coll Cardiol Img 2009;2:858–68.
5. Moreno PR. The high-risk thin-cap fibroatheroma: a new kid on the block. Circ Cardiovasc Interv 2009;2:500–2.

Intracardiac Echocardiographic Detection of Mobile Echodensities Adherent to the Intracardiac Leads

We read with interest the report by Naqvi et al. (1) describing the utility of real-time 3-dimensional (3D) transesophageal echocardiography in suspected right-side endocarditis in 3 patients with pacemaker (PM) or implantable cardioverter-defibrillator (ICD) leads and biological tricuspid prostheses. Precise detection and delineation of location of vegetation associated with intracardiac structure or leads in these patients may help therapeutic medical and surgical treatment decisions. Three-dimensional echocardiography has the potential to both complement existing 2-dimensional imaging modalities (transthoracic and transesophageal echocardiography) and enhance the ability to define the spatial location of the vegetation relative to a device lead or prosthetic valve and surrounding intracardiac structures, as indicated by Naqvi et al. (1). Although 3D echocardiography represents a rapidly evolving technology, it has definite limitations such as a relatively low spatiotemporal resolution, slow imaging acquisition rate, lack of standardized 3D views, and a steep learning curve in both understanding and appropriately integrating 3D images in a procedural environment (2,3).

In our experience with intracardiac echocardiography (ICE) in >2,000 ablation cases, it has also proved effective in real-time detection of mobile echodensities/thrombus adherent to the intracardiac PM or ICD (4). With the ICE transducer placed in the right atrium (RA) or right ventricle (RV), one can image the course of intracardiac leads from/in the RA (Fig. 1A) to the right atrial appendage (RAA) (Fig. 1B) and/or RV (Fig. 1C) and detect any mobile echodensity/thrombus attached to the intracardiac leads. In 86 consecutive patients with a PM or ICD who presented for atrial fibrillation or ventricular tachycardia ablation procedures, 26 of 86 patients (30%) had a mobile echodensity/thrombus (average length 18 ± 6 mm and width 4 ± 2 mm) attached to the intracardiac lead in the RA/RAA (n = 25) and/or RV (n = 5) identified with ICE.

ICE revealed mobile echodensities adherent to the intracardiac leads consistent with either thrombi, vegetation, or infected thrombi. The diagnosis of endocarditis related to PM/ICD lead infection should be suspected in the presence of fever, bacteremia, or pulmonary lesions consistent with a septic embolus. Compared with the 2 patients with recurrent infective endocarditis (fever, bacteremia, or perforation in the bioprosthetic tricuspid valve detected) presented by Naqvi et al. (1), our patients had no fever and were asymptomatic. We found an elevated pulmonary artery systolic pressure in the group who demonstrated a mobile echodensity/thrombus (5) compared with those with no echodensity/thrombus (n = 43) detected. No differences were found in the patient characteristics (e.g., age, sex), type of ablation, left

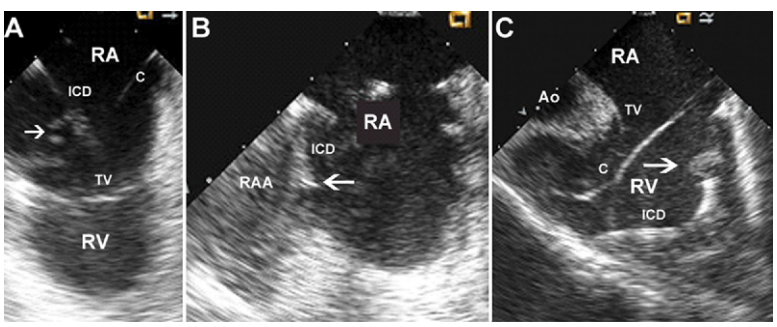

Figure 1. Intracardiac Echocardiographic Imaging of a Mobile Thrombus Attached to Intracardiac Leads

Intracardiac echocardiographic images with the transducer placed in the right atrium (RA), showing the mobile thrombus **(arrow)** attached at the implantable cardioverter-defibrillator (ICD) lead in the RA **(A)**, right atrial appendage (RAA) **(B)** or right ventricle (RV) **(C)**. Ao = aortic root; C = ablation catheter; TV = tricuspid valve.